

Prediction of Ductile Fracture Toughness

J.-S. Wang¹ and G. B. Olson^{1, 2}

¹QuesTek Innovations LLC, Evanston, USA; ²Northwestern University, Evanston, USA

Abstract

Inspired by recent multiscale modeling of void/microvoid interaction in ductile fracture, a new analysis of literature data on ultrahigh strength martensitic steels shows that J_{IC} toughness normalized by primary inclusion mean spacing is parabolically related to the measured critical primary void size ratio. Interpreting this critical ratio as a measure of the critical intervoid ligament strain for primary void coalescence by finer scale microvoid instability, calculation of the critical strain from Rice-Tracey void growth shows that J_{IC} toughness is exponentially related to the critical microvoid instability strain. This represents a far stronger sensitivity to critical strain than the previously assumed linear scaling. An approximate correlation of this critical strain to macroscopic fracture ductility allows an estimate of fracture toughness.

1. Introduction

Prediction of ductile fracture toughness, numerically or analytically, from microstructural and constitutive parameters has been a long-standing goal of the materials science and solid mechanics communities. Metallographic studies and recent multiscale simulations [1-6] show that 3D ductile fracture starts with plastic deformation followed by nucleation and growth of primary voids, and completes through primary void coalescence by a mechanism of intervoid ligament mechanical instability driven by interactive microvoiding on submicron-scale particles. New mechanistic insights provide an opportunity for reinterpretation of available literature data.

The mode I J-integral ductile fracture toughness is proportional to the critical crack tip opening displacement, δ_{1C} , and the flow stress σ_0 (usually taken to be the average of the yield strength and UTS) [7]:

$$J_{IC} = \frac{1}{d_n} \delta_{1C} \sigma_0$$

where $d_n \sim 0.6$ depending on material deformation properties. Rice and Johnson [8] were the first to relate the crack tip opening displacement, δ , to inclusion microstructure. Based on a rigorous mechanics analysis at the crack tip, they derived that the true strain ahead of a crack tip is a function of a parameter X/δ , where X is the distance of a material point from the tip before deformation. Adopting a simple idea that some critical matrix fracture strain must be achieved at a material point initially at a distance X_0 from the crack tip, they concluded from numerical calculations that

$$\delta_{IC} \sim 1.0 \text{ to } 2.7 X_0$$

and identified X_0 as the mean nearest neighbor spacing of primary inclusions responsible for ductile fracture.

Since X_0 and σ_0 are experimentally measurable, it is tempting that the ductile fracture toughness might be predicted from tensile test and inclusion analysis. A widely cited model in the literature is the Hahn-Rosenfield model [9], derived directly from the R-J model by using the correlations between J_{IC} and δ_{IC} , J_{IC} and K_{IC} , and taking $X_0 = (4\pi/3f)^{1/3} r$, where X_0 is defined as 3D spacing and f and r are the volume fraction and the mean radius of the primary inclusions, respectively.

A complete ductile fracture toughness model must include parameters related to both primary and secondary voids. Building on the Hahn-Rosenfield framework, Ritchie *et. al.* proposed that at the onset of ductile fracture the local equivalent plastic strain ahead of the crack tip must exceed a critical strain, ε_c , over a characteristic distance, l_0 , [10]. Based on this suggestion, J_{IC} for ductile fracture is

$$J_{IC} = \varepsilon_c l_0 \sigma_0$$

i.e., the ductile fracture toughness linearly relates to a critical strain ε_c . Further, Garrison proposed that the term $\varepsilon_c l_0$ is equivalent to the critical size of primary voids and the mean spacing of primary inclusions (X_0) such that [11-17]:

$$\varepsilon_c l_0 \sim X_0 \left(\frac{R}{R_0} \right)$$

which implies

$$\delta_{IC} \sim X_0 \left(\frac{R}{R_0} \right)$$

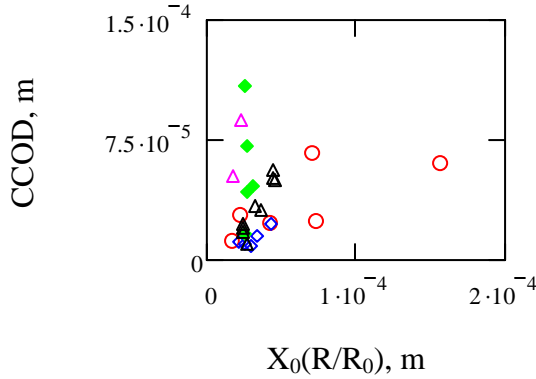
where R/R_0 is the ratio between the final dimple size and the mean size of the primary inclusions. The ductile fracture toughness can thus be related to the mechanical behavior of the material, the primary inclusion distribution and the measured growth of primary voids.

To check this relation, significant efforts were devoted to measure final dimple sizes at fracture surfaces of various types of steels. Based on data available in the literature [11-13, 18-25], the present work shows that the ductile fracture toughness normalized by the flow stress and the spacing of the primary inclusions is a power function of the void growth ratio R/R_0 , instead of the previously proposed linear relation. Applying the void growth law of Rice and Tracey [26], we conclude that the ductile fracture toughness is related exponentially, instead of linearly, to the critical strain ε_c , *i.e.*, exhibits a much stronger sensitivity to the critical strain. A stronger correlation of ductile fracture toughness is thus feasible by quantifying the critical level of primary void growth. Inspired by recent simulations of ductile fracture as a multiscale process [1-6], we also explore correlation of the critical primary void growth ratio with the critical strain for

finer scale microvoid localization, as estimated from measures of macroscopic fracture ductility.

2. Toughness and the void size

Garrison's proposed correlation between the critical crack tip opening and the parameter $X_0(R/R_0)$ is represented in Fig. 1. Examination of the figure suggests



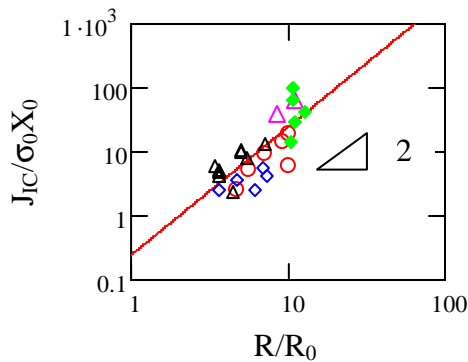
that a rough correlation may be found for each type of steel, but no collective correlation exists.

Figure 1 the critical crack tip opening displacement vs. $X_0(R/R_0)$. Red circle: AF1410, black triangle: AerMet100, blue diamond: UHS martensitic steels, green full diamond: HP9-4-10 and HP9-4-20 steels, open purple triangle: HY180. The symbols are the same in all figures

With multiscale dilatational plasticity constitutive models, relations between toughness and microstructural details have now been numerically calculated for ductile materials [1-6]. The main results of these studies suggest a dependence of the toughness on the initial microstructural parameters in a general form

$$\frac{J_{IC}}{\sigma_0 X_0} = F\left(\frac{\sigma_0}{E}, n, f, W_0, \lambda_0\right)$$

where E is Young's modulus, n is the apparent strain hardening exponent, W_0 and λ_0 are the shape and spacing parameters of the voids. Ignoring the shape effect, the data collected here show a simple power law correlation with critical void growth ratio represented in Fig. 2. The fracture toughness normalized by the flow stress and the spacing of primary inclusions is related in a power law to the ratio of the radius of the critical voids to the initial radius, R/R_0 , such that



$$\frac{J_{IC}}{\sigma_0 X_0} = C_0 \left(\frac{R}{R_0}\right)^p$$

Figure 2 The normalized ductile fracture toughness $J_{IC}/\sigma_0 X_0$ vs. the growth ratio of primary voids R/R_0 , showing the power law correlation

where C_0 is the value of $J_{IC}/\sigma_0 X_0$ at $R/R_0 = 1$. The initial radius of the voids, R_0 , is assumed as the radius of primary inclusions. Fitting the data in Fig. 2 finds that $C_0=0.23$, $p=2$. The parabolic dependence of ductile fracture toughness on the primary void growth ratio is thus stronger than the previously proposed linear scaling.

3. Void growth and the phenomenological toughness model

The proposed power law correlation suggests a dominant role of the critical value of the primary void growth ratio in ductile fracture. Rice and Tracey [26] were the first who proposed the constitutive growth law of void growth in an infinite solid under a remote tensile mean stress σ_m

$$\frac{\dot{R}}{\dot{\varepsilon}R} = C \exp\left(\frac{3\sigma_m}{2\sigma_0}\right)$$

where $\dot{\varepsilon}$ is the true strain rate and $C = 0.283$. The Rice-Tracey model predicts that the strain rate normalized void growth rate is an exponential function of the stress triaxiality, σ_m/σ_0 , at a distance from the crack tip where voids initiate. Integrating under constant strain rate, the Rice-Tracey model relates the void growth ratio to the strain ε in the matrix:

$$\frac{R}{R_0} = \exp\left[C\varepsilon \exp\left(\frac{3\sigma_m}{2\sigma_0}\right)\right]$$

Since the normalized ductile fracture toughness, $J_{IC}/\sigma_0 X_0$, is a power function of R/R_0 , the Rice-Tracey model suggests that ductile fracture toughness is an exponential function of the critical strain. The final value of R/R_0 is reached when the matrix strain ε reaches ε_c the critical strain for primary void coalescence, where the matrix is softened by secondary microvoids. This critical strain is then

$$\varepsilon_c = \frac{1}{C} \ln\left(\frac{R_c}{R_0}\right) \exp\left(-\frac{3\sigma_m}{2\sigma_0}\right)$$

Based on the Ritchie *et.al.* proposal, ductile toughness would then be linearly related to the critical strain and hence

$$\frac{J_{IC}}{X_0\sigma_0} \propto \ln\left(\frac{R}{R_0}\right)$$

A semi-logarithmic plot of the normalized J_{IC} vs. (R/R_0) is shown in Fig. 3. In contrast to the power law behavior demonstrated in Fig. 2, the proposed linear in the semi-logarithmic plot correlation does not appear.

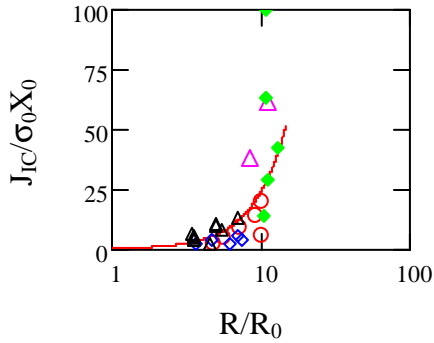


Figure 3 The normalized ductile fracture toughness $J_{IC}/\sigma_0 X_0$ vs. the growth ratio of primary voids, R/R_0 , in a semi-logarithmic plot

3D numerical simulations demonstrate that the stress triaxiality at the intervoid ligament varies during void growth [6]. A value of $\sigma_m/\sigma_0 \sim 2.1$ in the intervoid ligaments is typical at the onset of void coalescence. With the (R/R_0) data available,

the critical strain can then be calculated. The normalized ductile fracture toughness $J_{IC}/\sigma_0 X_0$ vs. the critical strain so obtained is shown in Fig. 4a. As expected, an exponential correlation is observed, such that

$$\frac{J_{IC}}{\sigma_0 X_0} = C_0 \exp(\alpha \epsilon_c)$$

where $C_0 = 0.23$ is the value of the normalized toughness at $\epsilon_c = 0$ and

$$\alpha = 2C \exp\left(\frac{3\sigma_m}{2\sigma_0}\right)$$

This leads directly to $\alpha = 13.208$, while data fitting to the computed ϵ_c of Fig. 4a gives $\alpha = 13.03$. The data exhibit a much stronger sensitivity of normalized toughness to critical strain than the previously proposed linear scaling. As shown by the log-log plot of Fig. 4b, a power law representation would correspond to a power of 3.5 compared to the value of 1 proposed by the old model.

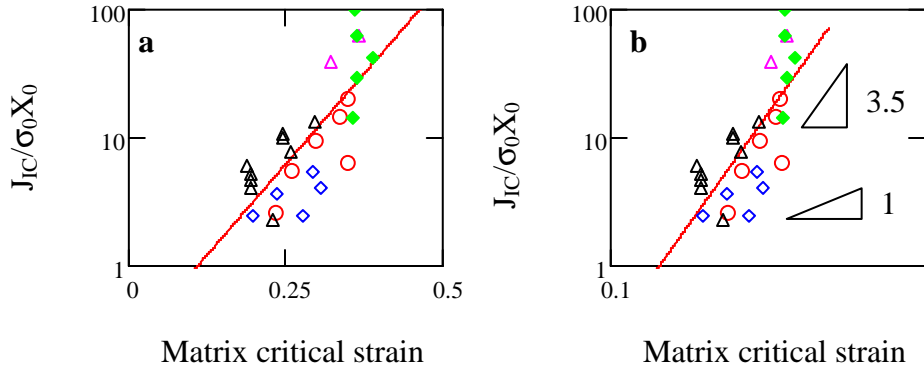


Figure 4 The normalized ductile fracture toughness $J_{IC}/\sigma_0 X_0$ vs. the matrix critical strain ϵ_c obtained based on Rice-Tracey growth model, a) semi-logarithmic plot showing the exponential correlation and b) double-logarithmic plot showing the far stronger dependence than linear

4. The matrix critical strain for ligament instability

The critical strain characterizes the onset of primary void coalescence, which consists of deformation localization at the microscale inside the intervoid ligament between neighboring primary voids. As discussed in detail in [1,2], depending on the position and orientation of the ligament relative to the principal straining axis, both normal separations and shear localizations are possible. Recent modeling has addressed the role of submicron particles in microvoid-driven localization of plastic deformation during ductile fracture [3-5]. The critical strain is greater if formation of secondary microvoids is delayed as the result of reducing secondary particle size and volume fraction.

Estimation of the matrix critical strain for microvoid instability from macroscopic fracture strain measures is confounded by the contributions of primary voiding in macroscopic fracture. The recent model of macroscopic fracture strain by Nahshon and Hutchinson accounts for the quantitative effects of both the stress triaxiality and strain state (*e.g.* plane strain vs. axisymmetric) as represented by

the third invariant of stress [27]. Measurements of instability strain in pure shear have the advantage of a reduced role of primary voiding and the plane strain condition of a crack tip, but are far removed from the triaxial tension stress state of mode I fracture. Fracture ductility data for uniaxial tension are more abundant and reflect the tensile stress state of a neck, but suffer from both a strong contribution from primary voiding and an axisymmetric strain state. Nonetheless, empirical correlation of the critical microvoiding strain measured by primary void growth with these macroscopic fracture ductility measures can provide a useful guide for estimating fracture toughness through our new correlations.

Data of instability strain under pure shear are available for the secondary hardened (stage IV temper) AF1410, AerMet100 steels and other ultrahigh strength martensitic steel under stage I and stage III tempering conditions as plotted against the modulus normalized UTS in Fig. 5a [28,29]. Based on these data a model of shear instability strain has been developed correlating with UTS and elastic properties as [30]

$$\gamma_{in} = \phi \exp\left(-\theta \frac{(1-\nu)\sigma_u}{E}\right)$$

where σ_u the UTS; E , Young's modulus; ϕ and θ are fitting constant for secondary hardening alloys and UHS low alloy steels under stage I temper conditions. Shear instability strain is related to the microstructure and strain hardening behavior as well as the UTS. The uniaxial tensile fracture strains are plotted in Fig. 5b. Both the shear instability strain and fracture strain in tension decrease with increasing UTS. This trend is expected to maintain for the matrix critical strain as supported by Fig. 5c.

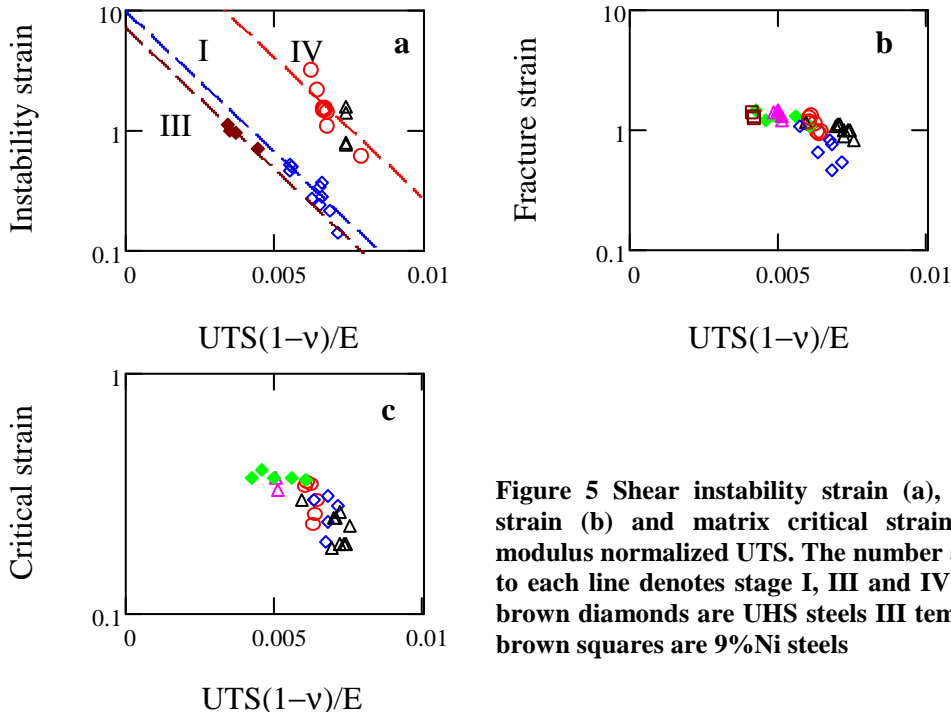


Figure 5 Shear instability strain (a), fracture strain (b) and matrix critical strain (c) vs. modulus normalized UTS. The number attached to each line denotes stage I, III and IV temper, brown diamonds are UHS steels III temper and brown squares are 9%Ni steels

The critical strain *vs.* the estimated shear instability strain and the measured fracture strain are plotted in Fig. 6a and b, respectively. In Fig. 6a, the stage I steels and secondary hardening steels form separated groups but a rough correlation between ϵ_c and γ_{in} can be found. In Fig. 6b, a linear correlation between the critical strain and tensile fracture strain is found ($\epsilon_c \cong 0.28\epsilon_f$), except for a few data points for stage I steels. Considering that fracture strain under plane strain conditions is in the range of 0.15~0.43 ϵ_f , the factor 0.28 is a reasonable value for the matrix stress triaxiality of 2.1 as adopted in the present work.

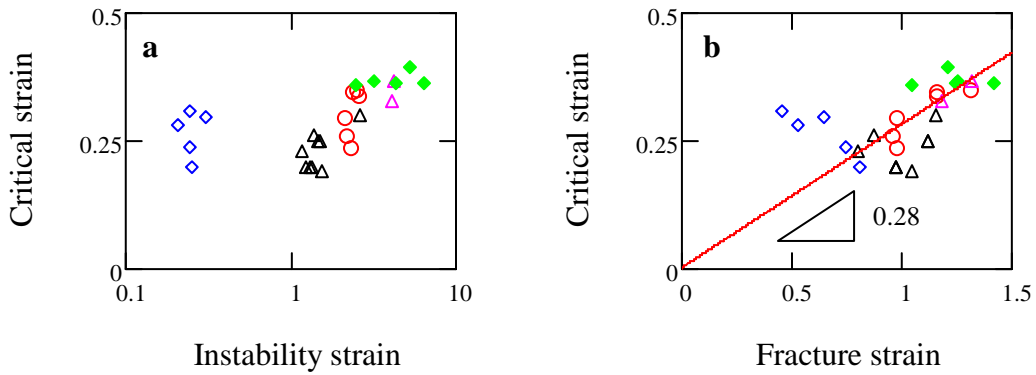


Figure 6 Critical strain vs. calculated instability strain in shear, a) and fracture strain, b)

As the critical strain is defined, it is feasible to estimate the ductile fracture toughness base on the phenomenological model. The results are shown in Fig. 7. Considering the approximation in the model and the experimental deviations, the estimated values by the phenomenological model are reasonably well consistent with the data.

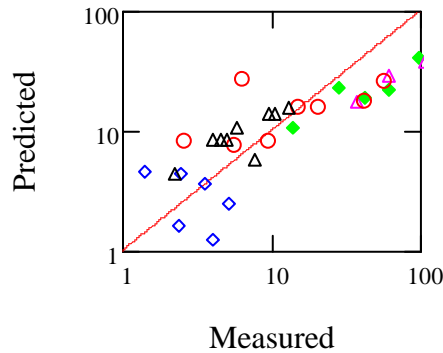


Figure 7 Estimate of the normalized ductile toughness based on the phenomenological model

5. Discussion

5.1. Ductile fracture toughness and the strength

The fracture toughness *vs.* the flow strength for the ultrahigh strength steels considered here are shown in Fig. 8, with the general trend that the toughness decreases with increasing strength. Despite the scaling of J_{IC} with σ_0 in Fig. 2, the

final behavior of Fig. 8 reflects a dominance of the strength dependence of γ_{in} , ε_f and ε_c , in Fig. 5.

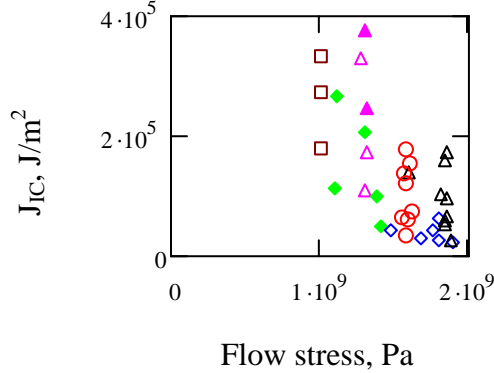


Figure 8 Fracture toughness vs. σ_0 . Additional data points are added. Brown square: 9%Ni steels and solid purple triangle: HY180 with Ti.

5.2. A phenomenological ductile fracture toughness model
A phenomenological ductile fracture model is derived as

$$\frac{J_{IC}}{\sigma_0 X_0} = C_0 \exp(\alpha \varepsilon_c)$$

and

$$\varepsilon_c = \beta \varepsilon_f$$

where $C_0=0.23$, $\alpha=13$, ε_f is the fracture strain in uniaxial tension and $\beta \sim 0.28$. Coalescence of primary voids is dominated by intervoid ligament instability. As the ductile fracture toughness is an exponential function of the critical strain, the critical strain thus plays a dominant role in ductile fracture toughness.

6. Conclusion

Based on a new analysis of literature data inspired by recent simulations, it is found that the ductile fracture toughness normalized by the flow stress and the spacing of the primary inclusions is a parabolic function of the critical primary void growth ratio. Solving a Rice-Tracey type equation under constant strain rate, the critical void growth ratio is an exponential function of the matrix critical strain for microvoid instability. This can in turn directly correlate the toughness with the critical instability strain and from this, a phenomenological model is suggested that the ductile fracture toughness is exponentially related to the critical strain, rather than a linear relation as previously assumed. The inverse strength dependence of this critical strain dominates the strength dependence of ductile fracture toughness. Control of the critical strain through microvoiding resistance is a significant opportunity for toughness enhancement.

Acknowledgement: This work is supported under the ONR/DARPA “D3D” Digital Structure Consortium Program, N00014-05-C-0241, Julie Christodoulou, Program monitor.

Reference:

- [1] T. Pardoen and J.W. Hutchinson, An extended model for void growth and coalescence, *J. Mech. Phys. Solids*, 48 (2000) 2467-2512
- [2] T. Pardoen and J.W. Hutchinson, Micromechanics-based model for trends in toughness of ductile metals, *Acta mater.*, 51 (2003) 133-148
- [3] S. Hao, B. Moran, W.K. Liu and G.B. Olson, A hierarchical multi-physics model for design of high toughness steels, *J. Computer-Aided Mater. Des.*, 10 (2003) 99-144
- [4] F.J. Vernerey, C. McVeigh, W.K. Liu, B. Moran, D. Tewari, D.M. Parks and G.B. Olson, The 3-D computational modeling of shear-dominated ductile fracture in steel, *JOM*, Dec. (2006), 45-51
- [5] F.J. Vernerey, W.K. Liu, B. Moran, and G.B. Olson, A micromorphic model for the multiple scale failure of heterogeneous materials, *J. Mech. Phys. Solids*, 56 (2008) 1320-1347
- [6] R. Tian and W.K. Liu, Northwestern University, private communications
- [7] C.F. Shih, Relationship between the J-integral and the crack opening displacement for stationary and extending cracks, *J. Mech. Phys. Solids*, 29 (1981) 305-326
- [8] J.R. Rice and M.A. Johnson, The role of large crack tip geometry changes in plane strain fracture, in M.F. Kanninen, W.F. Adler, A.R. Rosenfield and R.J. Jaffee (Eds.), *Inelastic Behavior of Solids*, McGraw-Hill, New York, 1970, pp. 641-672
- [9] G.T. Hahn and A.R. Rosenfield, Metallurgical factors affecting fracture toughness of aluminum alloy, *Metall. Trans.* 6A (1975) 653–668
- [10] R.O. Ritchie, W.L. Server, R.A. Wullaert, Critical fracture stress and fracture strain models for the prediction of lower and upper shelf toughness in nuclear pressure vessel steels. *Metall. Trans.* 10A (1979) 1557–1570
- [11] W.A. Garrison Jr., A microstructural interpretation of the fracture strain and characteristic fracture distance, *Scr. Met.*, 18 (1984) 583–586
- [12] W.A. Garrison Jr., A micromechanistic interpretation of the influence of undissolved carbides on the fracture toughness of a low alloy steel, *Scr. Met.*, 20 (1986) 633–636
- [13] W.M. Garrison Jr., The effect of silicon and nickel additions on the sulfide spacing and fracture toughness of a 0.4 carbon low alloy steel. *Metall. Trans.* 17A (1986) 669–678
- [14] W.M. Garrison and J.L. Maloney, Lanthanum additions and the toughness of ultra-high strength steels and the determination of appropriate lanthanum additions, *Mater. Sci. Eng.* 403A (2005) 299-310
- [15] J.L. Maloney, W.M. Garrison, The effect of sulfide type on the fracture behavior of HY180 steel, *Acta Mater.*, 53 (2005) 533-551
- [16] L.E. Iorio and W.M. Garrison, The effects of titanium additions on AF1410 ultra-high-strength steel, *Met. Mat. Trans.* 37A (2006) 1165-1173
- [17] W.A. Garrison, A.L. Wojcieszynski, A discussion of the effect of inclusion volume fraction on the toughness of steel, *Mat. Sci. Eng.* A464 (2007) 321-329

- [18] W.M. Garrison Jr. and K.J. Handerhan, Effects of rare earth additions on the mechanical properties of the secondary hardening steels AF1410, *Scr. Met.*, 22 (1986) 409-412
- [19] W.A. Garrison Jr. N.R. Moody, Ductile Fracture, *J. Phys. Chem. Solids* 48 (1987) 1035-1074
- [20] W.M. Garrison Jr., N.R. Moody, The influence of inclusion spacing and microstructure on the fracture-toughness of the secondary hardening steel AF1410, *Metall. Trans.*, 18A (1987) 1257 -1263
- [21] K.J. Handerhan, W.M. Garrison Jr., N.R. Moody, A comparison of the fracture-behavior of 2 heats of the secondary hardening steel AF1410, *Metall. Trans.* 20A (1989) 105-123
- [22] K.J. Handerhan, W.M. Garrison Jr., A study of crack tip blunting and the influence of blunting behavior on the fracture-toughness of ultra-high strength steels, *Acta Metall. Mater.*, 40 (1992) 1337-1355
- [23] J.W. Bray, K.J. Handerhan, W.M. Garrison Jr., A.W. Thompson, Fracture-toughness and the extents of primary void growth, *Metall. Trans.* A23 (1992) 485-496
- [24] Koji Sato, Improving the toughness of ultrahigh strength steel, Ph. D. dissertation, U. C. Berkeley, 2002
- [25] Li Jie, Guo Feng, Li Zhi, Wang Jun-li, Yan Ming-gao, Influence of sizes of inclusions and voids on fracture toughness of ultra-high strength steel AerMet100, in *Proceedings of Sino-Swedish Structural Materials Symposium 2007*, pp254-258
- [26] J.R. Rice, D.M. Tracey, On the ductile enlargement of voids in triaxial stress fields, *J. Mech. Phys. Solids* 17 (1969) 201–217
- [27] K. Nahshon and J.W. Hutchinson, Modification of the Gurson model for shear failure, *Euro. J. Mechanics A/Solids* 27 (2008) 1-17
- [28] J.G. Cowie, M. Azrin, and G.B. Olson, Microvoid formation during shear deformation of ultrahigh strength steels, *Metall. Trans.*, 20A (1989) 143-153
- [29] J.H. Graves and J.H. Beatty, Ballistic performance and Adiabatic shear behavior of AerMet100 steel, ARL-TR-454, 1994
- [30] J.-S. Wang and G.B. Olson, unpublished work